THEORY OF FLUORESCENCE DEPOLARIZATION OF DIMERS FROM THE NONLINEAR SCHRÖDINGER EQUATION ☆

V.M. KENKRE and G.P. TSIRONIS [1]
Department of Physics and Astronomy, University of New Mexico, Albuquerque, NM 87131, USA

Strong interactions with vibrations give rise to nonlinearities in the transfer of energy or excitation in quantum systems, with resulting polaronic and solitonic phenomena. With the help of exact solutions of a discrete nonlinear Schrödinger equation obtained recently for a two-site system, we study the effects of such nonlinearities in fluorescence depolarization experiments. The system investigated is a collection of noninteracting molecular dimers subjected to a linearly polarized light beam of variable orientation (of the polarization direction), and the observable studied is the degree of polarization of fluorescence emitted by the dimers. Results differing substantially from their linear counterparts are shown to emerge, and clear manifestations of nonlinearity are predicted.

1. Introduction

This paper is one in a series of investigations undertaken to gain insights into the effects that nonlinearity in the evolution of quantum systems can have on experimentally observable quantities. When a quasiparticle or excitation in a solid (an electron, an exciton, or even an interstitial atom) interacts strongly with the vibrations of the solid, the behaviour of the quasiparticle or excitation can undergo profound modifications. A particularly interesting example of such a modification is the onset of nonlinearities in the transport equation for the quasiparticle. Such an equation is typified by

$$dc_m(t)/dt = -i \sum_n V_{mn} c_n + i\chi |c_m|^2 c_m . \quad (1.1)$$

This "discrete nonlinear Schrödinger equation" [1–3] describes the time evolution of c_m, the amplitude for the quasiparticle to be in the Wannier state $|m\rangle$ localized on site m of the crystal under study, V_{mn} is the intersite matrix element describing the transfer of the quasiparticle from state $|n\rangle$ to state $|m\rangle$, and χ

is the nonlinearity parameter expressed as the energy lowering due to polaronic effects. We put $\hbar = 1$ throughout this paper. In the absence of the nonlinearity χ, (1.1) becomes the familiar (linear) Schrödinger equation which, along with the master equation and the generalized master equation that it gives rise to [3] under strong interactions with reservoirs, has been used to interpret transport in a variety of situations. The nonlinear equation (1.1) in the presence of χ is, however, profoundly different in nature from its linear counterpart. One of the differences is that (1.1) supports soliton solutions [1,2]. another is that it possesses [4] built-in polaronic features [5–7] not present in the linear counterpart. There are two kinds of questions concerning (1.1) that are of current interest. One has to do with the validity of the assumptions made and procedures employed in the derivation of (1.1) for given Hamiltonians [1,8,9]. The other is concerned with the elucidation of the effects of the nonlinearities inherent in (1.1) on specific experimental observations [4,10,11]. Our interest here lies in the second of these two questions, i.e. in the investigation of *observable* effects of the nonlinearities of (1.1). In the first paper [10] of this series we analyzed neutron scattering. In the present paper we investigate fluorescence depolarization.

The system under investigation here is a variable-distance noninteracting donor–acceptor pair of molecules [12]. A practical example is provided by the so-called "stick-dimers" in which poly-L-proline oligomers of controllable length are used to separate an α-naphthyl group at the carboxyl end – the donor – from the dansyl group at the imino end – the acceptor –, and the efficiency of energy transfer is studied through measurements of fluorescence excitation, emission and polarization spectra. For the analysis in the present paper, we shall take the donor and the acceptor to be identical molecules. On illumination, either of the molecules in the pair may undergo electronic excitation. The direction of the transition dipole moment produced on the molecule through the process of excitation depends on geometrical factors and is generally different for the two molecules in the pair. For simplicity we will assume the two dipole moments to be coplanar and mutually perpendicular. One could, in principle, create an excitation of the dimer which is localized on one of the two molecules by shining (broad-band) light polarized in the direction of the dipole moment on that molecule. Varying the angle of the polarization of the incident light beam would result in varying the relative amplitude or probability of excitation of either molecule. if $I_\parallel$ and $I_\perp$ are the intensities of fluorescence polarized respectively parallel and perpendicular to the direction of the polarization of the incident light, the degree of fluorescence polarization f, given by

$$f = (I_\parallel - I_\perp)/(I_\parallel + I_\perp) , \tag{1.2}$$

is clearly a convenient experimental observable for the investigation of excitation transfer within the dimer. A detailed presentation of the formalism required for the analysis of these observations has been given by Rahman et al. [13]. It is clear that the intensity of fluorescence in the direction of the unit vector e_λ is given by

$$I_\lambda = \sum_{m,n} \rho_{mn} (\boldsymbol{\mu}_m \cdot e_\lambda)(\boldsymbol{\mu}_n \cdot e_\lambda) , \tag{1.3}$$

where the $\boldsymbol{\mu}$ are the dipole moments, ρ are the matrix elements of the density matrix, and m,n represent states in a suitable basis. If the basis is that of localized states, m and n are the molecular (site) states 1 and 2 of the electronic excitation. If the basis is that of "momentum" states, m and n are the symmetric and antisymmetric combinations of the site states, respectively. With the understanding that ϕ is the angle made by the polarization of the incident light with the transition dipole moment on molecule 1, we can at once write $\boldsymbol{\mu}_1 \cdot e_\parallel = \boldsymbol{\mu}_2 \cdot e_\perp = \cos \phi$ and $\boldsymbol{\mu}_1 \cdot e_\perp = -\boldsymbol{\mu}_2 \cdot e_\parallel = -\sin \phi$. This results in the following expression for the degree of fluorescence depolarization f in terms of the density matrix elements of the dimer:

$$f = p \cos 2\phi + r \sin 2\phi . \tag{1.4}$$

Here p and r are given by the following combinations of the density matrix elements in the site representation:

$$p = \rho_{11} - \rho_{22}, \quad r = \rho_{12} + \rho_{21} . \tag{1.5}$$

Unfortunately, the symbol p has been used in earlier publications to denote two different quantities, both of which appear in intimate juxtaposition in our present analysis: the degree of fluorescence polarization in publications such as ref. [13], and the probability difference in the dimer in our previous papers on this subject such as refs. [4,10,11]. We have found it convenient to keep to the latter usage (see (1.5)) here and to use the symbol f (see (1.4)) for the degree of fluorescence polarization. We hope that the notation we have adopted will minimize the confusion.

The experimental investigation into the effects of nonlinearity on energy transfer through fluorescence depolarization probes thus consists in the measurement of f as a function of one or more of several variables: time t, the angle ϕ, or some other parameter such as the distance between the molecules in the dimer. We will concentrate our attention in this paper primarily on the behavior of the steady state f as a function of the angle ϕ.

Our paper is organized as follows. In section 2 we present the exact solutions of p and r for arbitrary initial conditions in the nonlinear dimer and combine them with (1.4) to derive the basic expression for the degree of fluorescence polarization in the dimer. In section 3 we exhibit the novel consequences of that expression for fluorescence depolarization experiments in the steady state. The specific quantity we calculate, plot, and discuss is the normalized steady-state degree of fluorescence polarization f_s, defined as

$$f_s = \frac{1}{\tau} \int\limits_0^\infty dt\, e^{-t/\tau} f(t)\,, \tag{1.6}$$

τ being the lifetime of the excitation. A discussion of the origin of the striking features of the plots shown forms the content of section 4. That section examines the physics of the interplay of nonlinearity with initial conditions in the dimer. Additional results of our analysis are presented in section 5 along with concluding remarks. The results include plots for time-dependent f, which would be of interest to time-resolved experiments such as those employing transient absorption spectroscopy, and plots for steady-state f_s averaged over orientations, which would be relevant to experiments on solutions or random systems.

2. Consequences of the nonlinear transfer of excitation

As our interest lies in the dimer, we take m,n in (1.1) to assume values 1 and 2 only. Thus, (1.1) takes the form

$$i\, dc_1/dt = Vc_2 - \chi|c_1|^2 c_1\,, \tag{2.1}$$

$$i\, dc_2/dt = Vc_1 - \chi|c_2|^2 c_2\,. \tag{2.2}$$

The first term in each of the two equations (2.1) and (2.2) describes the transfer of excitation between the two sites of the dimer in an oscillatory fashion with a frequency proportional to V. The second term describes the tendency of the excitation to lower its energy (and thereby invite the phenomenon of self-trapping) by an amount proportional to χ as a result of its interactions with the vibrations. Some of the fascinating consequences of the combined action of these two terms have been discussed in our recent work [4,10,11], to which we refer the reader for pertinent details. For the analysis of fluorescence depolarization of interest to the present paper we require the quantities p and r defined in (1.5). We obtain them as follows.

Eqs. (2.1) and (2.2) yield [4] a closed equation for p, the difference in the occupation probabilities at the two sites:

$$d^2p/dt^2 = Ap - Bp^3\,. \tag{2.3}$$

The constants A and B are determined not only by the dimer parameters V and χ representing the intersite transfer and the interaction with the vibrations respectively, but also by initial conditions, i.e. by the values of the density matrix elements at the initial time:

$$A = \tfrac{1}{2}\chi^2 p_0^2 - 4V^2 - 2V\chi r_0\,, \quad B = \tfrac{1}{2}\chi^2\,. \tag{2.4}$$

The subscript 0 denotes the initial value (at $t=0$). The general solution of (2.1) is given by [4,10,11]

$$p(t) = C\, \text{cn}[(C\chi/2k)(t-t_0)|k]$$
$$= C\, \text{dn}[(C\chi/2)(t-t_0)|1/k]\,, \tag{2.5}$$

$$1/k^2 = 2 + (1/C^2)$$
$$\times [(4V/\chi)^2 + (8V/\chi)r_0 - 2p_0^2]\,, \tag{2.6}$$

where C and t_0 are arbitrary constants that are easily determined from the initial conditions. Details of the general expressions for these constants will not be required in the following but may be found in our earlier work [11, eqs. (A-13), (A-15)]. Although the cn and dn (elliptic) functions in (2.5) are interrelated through the well-known Jacobi (real) reciprocal transformation [14], normal usage represents the function as cn if $k \leqslant 1$ and as dn if $k \geqslant 1$.

Eq. (2.5) is the required expression for p. In order to obtain an expression for r, the sum of the off-diagonal elements of the density matrix as defined in (1.5), we manipulate (2.1), (2.2) to obtain

$$dp/dt = i2V(\rho_{12} - \rho_{21})\,, \tag{2.7}$$

$$dr/dt = i\chi p(\rho_{12} - \rho_{21})\,. \tag{2.8}$$

The elimination of $\rho_{12} - \rho_{21}$ from (2.7) and (2.8) allows one to express $r(t)$ at all times t completely in terms of its own initial value r_0 and of the probability difference $p(t)$:

$$r(t) = r_0 + (\chi/4V)(p^2 - p_0^2) \tag{2.9}$$

The substitution of (2.9) in (1.4) gives

$$f(t) = (\cos 2\phi)p(t)$$
$$+ (\sin 2\phi)\{r_0 + (\chi/4V)[p^2(t) - p_0^2]\}\,. \tag{2.10}$$

Eq. (2.10) is our point of departure for the investigation of fluorescence depolarization in dimers. The observable f may be time dependent or steady state. If it is the former, we use the time-dependent value

of $p(t)$ to calculate it. If it is the latter, we use the integration in (1.6) to calculate the steady-state value f_s. The initial condition inherent in the illumination determines the angle ϕ and the values of r_0 and p_0. The dimer and its interaction with the vibrations provide the values of V and χ.

The novel features in fluorescence depolarization to be presented below stem from the nonlinearities in the transfer of the excitation. That the time dependence of $f(t)$ can be changed profoundly from what it would be in the absence of nonlinearity may be appreciated from (2.5), which, on being substituted in (2.10), yields $f(t)$. The new features that emerge are of two kinds. The first arise from the fact that the Jacobian evolution of $p(t)$ is far richer than the trigonometric evolution characteristic of the linear Schrödinger equation, one of its consequences being the transition [4,10] from "free" to "self-trapped" motion of the excitation. Thus, for sufficient degree of nonlinearity, the oscillations of $p(t)$, which would appear on both sides of 0 if the dimer were linear, are restricted to one side only. Excitation transfer then proceeds as in a *nonresonant* linear dimer. Features of this kind can be seen also in previously studied experimental observables such as scattering functions [11]. The second kind are peculiar to fluorescence depolarization observations, and involve new effects not discussed earlier. They arise from the interplay of the nonlinearities in the transfer of excitation with certain initial conditions possible in fluorescence depolarization experiments, and may be detected, in principle, in steady-state observations. They are emphasized in this paper.

3. The degree of fluorescence polarization

The basis of our study of steady-state fluorescence depolarization experiments is expression (2.10) derived above from the time-dependent degree of fluorescence polarization $f(t)$, the general result (2.5), (2.6) for the probability difference $p(t)$, and the prescription (1.6) to calculate the steady-state f. Eq. (1.2) describes the experimental meaning of f.

In fig. 1 we plot $f_s(\phi)$ calculated from (1.6) as a function of the polarization angle ϕ for various degrees of the nonlinearity parameter χ. For $\chi/4V=0$, the system is linear and the integrated signal varies
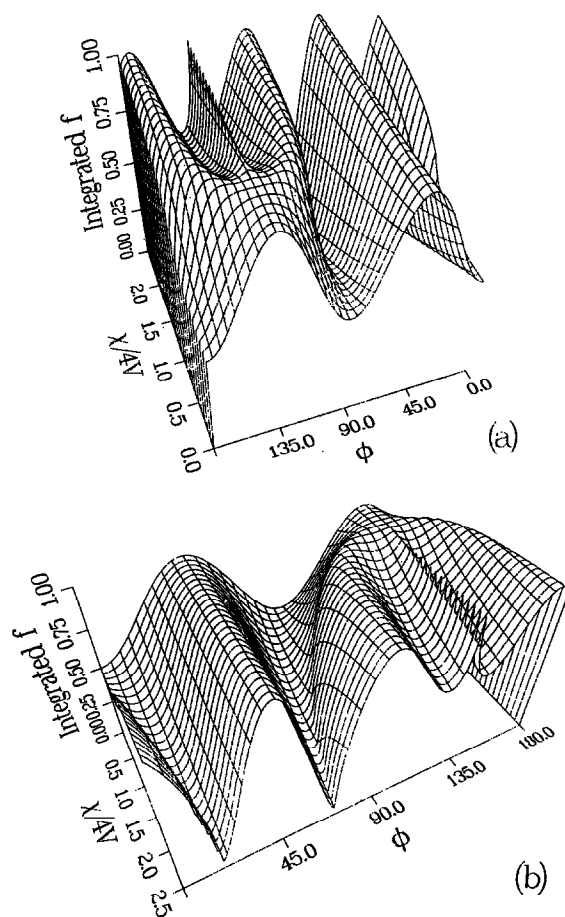

Fig. 1. Effects of nonlinearity on the integrated (steady-state) degree of fluorescence polarization f_s: f_s is plotted along the z axis as a function of the angle of polarization ϕ (in deg) along the x axis and as a function of the nonlinearity ratio $\chi/4V$ along the y axis. (a) and (b) are simply opposite views of the f–ϕ–χ surface. The linear limit $\chi=0$ is clear in the foreground in (a) and the result of large nonlinearities in (b). Of special mention are (i) the value $\chi/4V=\frac{1}{2}$ at which one encounters a transition in the f–ϕ dependence, (ii) the shift of the f–ϕ maximum as one moves along the $\chi/4V$ axis, and (iii) a "pinning" of the f–ϕ curve at 135°. We have taken $2V\tau=1$ in all the figures for simplicity.

sinusoidally as a function of the polarization angle ϕ. As χ takes on non-zero values, minor changes occur in this variation for small nonlinearities. However, beyond a critical value of χ, the curve changes qualitatively and pronounced new effects are seen around $\phi=135°$. Figs. 1a and 1b show a three-dimensional representation of the variation of f_s from opposite views. The linear limit is made clear by the former

and the new effects of the nonlinearity by the latter. The simple sinusoidal variation of $f_s(\phi)$ is seen facing the viewer in fig. 1a. The changes brought about by nonlinearity are trivial until the ratio $\chi/4V$ equals $\frac{1}{2}$. Peculiar dips now appear in the f curve and there seems to be a "pinning" of the curve at 135°. The effects are not dramatic in the right half of the curve, i.e. around 45°. Fig. 1b shows the opposite view, brings the high-χ portion of the f curve into the foreground, and makes it easier to appreciate the effects on nonlinearity. The pinning and related aspects of the variation on f are clearly visible.

The projection of the f–ϕ–χ surface on the f–ϕ plane is shown in fig. 2. Curves a, b, c, d, e represent various values of the nonlinearity ratio $\chi/4V$: 0, 0.2, 0.5, 1, and 1.5. Curve a ($\chi=0$) shows the simple sinusoidal variation characteristic of a linear dimer. Curve b shows a trivial change in the variation brought about by the nonlinearity while the dimer is still in the "free" region. Curve c ($\chi=2V$) shows the transition to self-trapped behavior. A flattening of the dependence of f on ϕ is characteristic of the transition and is apparent in curve c. Curves d and e show the dramatic effects
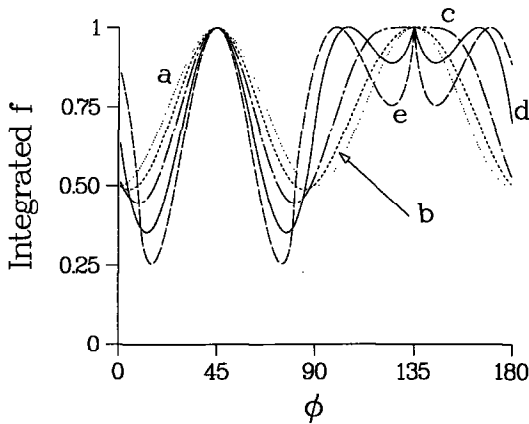

Fig. 2. Effects of nonlinearity of f_s: projection of the f–ϕ–χ surface in fig. 1 on the f–ϕ plane. Curves a, b, c, d, e, represent various values of the nonlinearity ratio $\chi/4V$: 0, 0.2, 0.5, 1, and 1.5, respectively. Curve a ($\chi=0$) shows the simple sinusoidal variation characteristic of a linear dimer. Curve b shows a trivial change in the variation brought about by the nonlinearity while the dimer is still in the "free" region. Curve c ($\chi=2V$) shows the transition to self-trapped behavior. A flattening of the dependence of f on ϕ is characteristic of the transition and is apparent in curve c. Curves d and e show the dramatic effects of nonlinearity: the shift of the maximum away from 135° and the "pinning" at 135°.

of nonlinearity: the shift of the maximum away from 135° and the "pinning" at 135°.

The consequences of nonlinearity that our analysis has predicted are thus:

(i) the slight variation of $f(\phi)$ with χ in the region $\chi<2V$;

(ii) the transition at $\chi=2V$;

(iii) the shift of the maximum away from $\phi=135°$, and

(iv) the cusp at 135°.

In order to understand how these features arise from the nonlinear Schrödinger equation, it is first necessary to appreciate, in a general way, the rather bizarre effects that the interplay on nonlinearity with initial conditions can have in the dimer. We describe these in section 4.

4. Origin of the new features in fluorescence depolarization

Consider eq. (2.5), which allows one to analyze the initial condition problem in complete generality, and make the simplifying assumption that $(\mathrm{d}p/\mathrm{d}t)_0=0$. This assumption is equivalent to placing the dimer initially in a pure state characterized by *real* off-diagonal matrix elements of the density matrix ρ. Eqs. (2.5) and (2.6) reduce to

$$p(t)=p_0\,\mathrm{cn}(p_0\chi t/2k|k)$$
$$=p_0\,\mathrm{dn}(p_0\chi t/2|1/k)\,, \tag{4.1}$$

$$k^2=k_0^2 p_0^2/(1+2k_0 r_0)\,, \tag{4.2}$$

k_0 being the nonlinearity ratio $\chi/4V$. The initial (real) amplitudes $c_1(0)$ and $c_2(0)$ can have either the same sign or opposite signs and correspond, respectively, to the relations $r_0=+(1-p_0^2)^{1/2}$ and $r_0=-(1-p_0^2)^{1/2}$ between the initial values of r and p. Let us examine the latter case. If the initial condition and the dimer parameter ratio k_0 are in the relation

$$k_0=\chi/4V=\tfrac{1}{2}(1-p_0^2)^{-1/2}\,, \tag{4.3}$$

we see that the elliptic parameter k^2 becomes infinite and the probability of occupation of the two sites is independent of time for all t! A further increase of the nonlinearity parameter χ beyond the value corresponding to (4.3) makes k^2, as given in (4.2), *negative*, and has quite unexpected consequences for the

time evolution of the dimer [15]. One normally expects that, in the initial stages of the probability oscillation, the site with the larger initial probability of occupation would become depopulated and that the other site would gain in population. Precisely the opposite effect is produced in the present case as a result of the combined action of the nonlinearity and the initial condition. The excitation seems to be "repelled", i.e. the site with the larger initial probability of occupation becomes even more populated. As the oscillation proceeds, the probability of the site with the initially larger occupation never decreases below that initial value. Fig. 3 depicts this behavior.

The fact that the elliptic parameter k^2 can become infinite for the condition (4.3) and negative for higher values of the nonlinearity contains the essential physics responsible for the peculiarities of the fluorescence depolarization curve of figs. 1 and 2. The case of (4.3) describes a situation in which the initial condition corresponds to the excitation being placed initially in a *stationary state* of the nonlinear dimer. The stationary states (the symmetric and antisym-
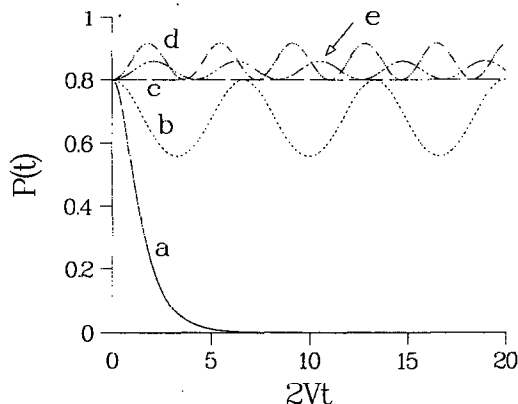

Fig. 3. The time dependence of the probability difference $p(t)$ in a nonlinear dimer for the initial condition $(dp/dt)_0 = 0$ and $r_0 = -(1-p_0^2)^{1/2}$, shown to illustrate the unexpected effects that can arise from the interplay of nonlinearities and initial conditions. All curves shown are in the self-trapped region and the respective values of $k_0 = \chi/4V$ are: (a) 0.625, (b) 0.7, (c) 0.833, (d) 0.9, and (e) 1.0. Curve c represents the coincidence of the initial state and a stationary state of the nonlinear dimer. Curves d and e exhibit the striking "repulsion" effect – see text – wherein the site with the initially larger probability of occupation *increases* in population. Curve c corresponds to the elliptic parameter k in (2.5) becoming infinite, and curves d and e to k becoming imaginary.

metric one) of the *linear* resonant dimer are characterized by the site-state amplitudes c_1 and c_2 given by $1/\sqrt{2}$, $1/\sqrt{2}$ for the symmetric state and by $1/\sqrt{2}$ for the antisymmetric state, respectively. The two states therefore possess resultant dipole moments which make respectively the angles $45°$ and $135°$ with the dipole moment of molecule 1. At these values of the angle of polarization ϕ, the excitation would find itself initially (and consequently for all time) in a stationary state. The steady-state quantity f_s would then be unity. Curve a of fig. 2 indeed shows that, for $\chi = 0$, f_s is unity at these stationary state angles $45°$ and $135°$.

As χ takes on values which are different from zero, but still smaller than $2V$, the stationary-state angles remain identical to those of the linear dimer. Consequences of nonlinearity exist but are not significant. Correspondingly, the $f-\phi$ dependence in figs. 1 and 2 undergoes only slight modifications from their linear limit. However, when $\chi = 2V$, the characteristic effects of nonlinearity set in. Putting $d^2p/dt^2 = 0$ in (2.3) gives us the stationary states of the nonlinear dimer [10,11]. From the right-hand side of (2.3) we see that we obtain two solutions for p. The first has $p = 0$ and corresponds to the trivial stationary state with equal occupation of the two site states. This state is reflected in figs. 1 and 2 in the fact that the peak at $45°$ is maintained for all values of the nonlinearity. For $\chi > 2V$, however, a second stationary state appears in the nonlinear dimer [10,11,16]. This state is responsible for the novel features of figs. 1 and 2. The site amplitudes in this state are quite different and represent self-trapping:

$$c_1 = (1/\sqrt{2})\{1 + [1-(2V/\chi)^2]^{1/2}\}^{1/2}, \qquad (4.4)$$

$$c_2 = (1/\sqrt{2})\{1 - [1-(2V/\chi)^2]^{1/2}\}^{1/2}. \qquad (4.5)$$

For values of χ in excess of $2V$, the nonlinear dimer acts like a *non-resonant* (linear) dimer. The site amplitudes in the stationary are clearly unequal and the resultant dipole moment of the stationary state, which was at $135°$ to the direction of that of molecule 1, now slips away from that orientation. The value of χ determines the amount of this slipping. Curves d and e in fig. 2 show this slipping or shift of the f maximum which, as we have discussed above, represents the stationary state.

The pinning effect at $135°$ occurs as a result of con-

flicting symmetries in the nonlinear dimer. Whenever the transition to self-trapping occurs, the nonlinear dimer takes on the behavior of a nonresonant (linear) dimer. A true linear nonresonant dimer does not have its stationary state dipole moment at 135° and possesses no symmetry around that angle. The equations of motion (2.1) and (2.2) on the other hand favor no site or angle, and the nonlinear dimer does possess complete symmetry around 135°. It is thus the combination of this symmetry requirement around 135° and the shift of the $f(\phi)$ peak stemming from the shift of the stationary state that is responsible for the appearance of the peculiar cusp in figs. 1 and 2.

It might be useful to point out here why the relevant nonlinearity ratio in our earlier work [4,10,11], viz. $\chi/4V$, is different from the ratio $\chi/2V$ that we have been discussing in the present paper. The former value describes the onset of a *dynamic* transition from free to self-trapped behavior, given a situation in which the excitation is completely localized on one of the sites initially. The latter value, on the other hand, describes a *static* transition at which the stationary states of the dimer change character. The dynamic transition is relevant to observables such as the neutron scattering function and the static transition to steady-state fluorescence depolarization.

5. Concluding remarks

The interaction of quasiparticles or excitations in solids with molecular or lattice vibrations can lead to a number of strong and discernible effects on transport phenomena. Traditionally, these interactions have been studied with the help of scattering, dressing and polaronic concepts. A new theoretical tool has appeared in the literature recently: the nonlinear Schrödinger equation pioneered for excitation transport by Davydov and others [1,2,17]. We believe it is of crucial current importance to explore the consequences of the interaction of excitations with vibrations with the help of this tool. The present paper contains the results of such an exploration.

We have applied our exact theory of the nonlinear dimer to a specific class of experiments in this paper and have shown that effects which are qualitatively new and experimentally discernible, at least in principle, do appear as clear consequences of the nonlinear Schrödinger equation. These are polaronic effects which, in spatially extended systems, could be further accompanied by solitonic phenomena. The experimental observation of the effects we have predicted requires the construction of appropriate dimers and their study in systems in which their orientation is not random. The construction of suitable systems with definite orientations of the dimers may turn out to be a difficult undertaking. We hope the present analysis will motivate experiments along this line. While awaiting those experiments, we have also carried out an analysis of the effects of nonlinearity in solution systems which are much easier to construct in the laboratory. The analysis performs an average over the orientations and therefore loses most of the clear manifestations of nonlinearity. We present the results graphically in fig. 4. The units of the averaged steady-state f_s are arbitrary. The abscissa is $\chi/4V$ and would correspond in the experiment to an appropriate power of the intermolecular distance in the dimer. It would not be difficult to carry out such an experiment with presently available techniques since the variation of the length of the "stick dimers" can be achieved by changing the number of the inert molecules separating the active end molecules of the stick dimer. We also present in fig. 5 the results of our analysis for time-dependent f. The simple oscillation
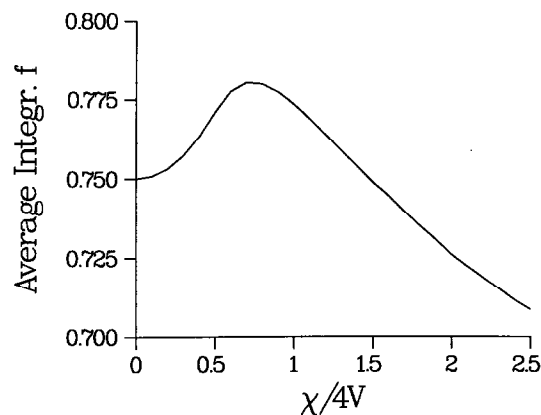

Fig. 4. The average over angles ϕ of the integrated (steady-state) degree of fluorescence depolarization f_s plotted as a function of the nonlinearity ratio $\chi/4V$. The system of interest here is a solution in which the dimers are oriented at random and the abscissa corresponds to an appropriate power of the intermolecular distance, i.e. of the "length" of the dimer.
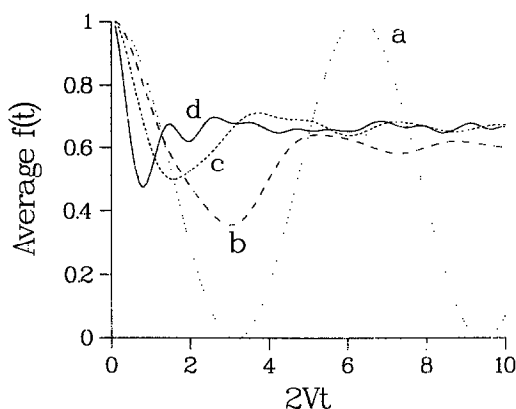
Fig. 5. The time dependence of $f(t)$ shown for various values of the nonlinearity. An apparent damping and a shift of the long-time limit of $f(t)$ are seen as consequences of nonlinearity.

characteristic of the linear dimer (curve a) is seen to undergo an apparent damping, and a shift of the value of the limit of $f(t)$ as $t \to \infty$. Relevant observations would involve time-resolved experiments on the picosecond and subpicosecond scales, and could employ transient absorption spectroscopy. The primary focus of the present paper being steady-state observations, however, we defer detailed comments on figs. 4 and 5 to a future publication.

Acknowledgement

References

[1] A.S. Davydov, J. Theoret. Biol. 38 (1973) 449; Soviet Phys. Usp. 25 (1982) 898, and references therein.

[2] A.C. Scott, F.Y. Chu and D.W. McLaughlin, Proc. IEEE 61 (1973) 1443.

[3] V.M. Kenkre, in: Exciton dynamics in molecular crystals and aggregates, ed. G. Höhler (Springer, Berlin, 1982).

[4] V.M. Kenkre and D.K. Campbell, Phys. Rev. B 34 (1986) 4959.

[5] T.D. Holstein, Ann. Phys. 8 (1959) 325, 343.

[6] D. Emin, Phys. Today 35 (1982) 34, and references therein.

[7] Y. Toyozawa, in: Organic molecular aggregates, eds. P. Reineker, H. Haken and H.C. Wolf (Springer, Berlin, 1983), and references therein.

[8] P.S. Lomdahl and W.C. Kerr, in: Physics of many particle systems, ed. A. Davydov, unpublished results.

[9] D.W. Brown, K. Lindenberg and B.J. West, Phys. Rev. A 33 (1986) 4104, 4110.

[10] V.M. Kenkre and G.P. Tsironis, Phys. Rev. B 35 (1987) 1473.

[11] V.M. Kenkre, G.P. Tsironis and D.K. Campbell, in: Nonlinearity in condensed matter, eds. A.R. Bishop, D.K. Campbell, P. Kumar and S.E. Trullinger (Springer, Berlin, 1987) p.226.

[12] S. Stryer and R.P. Haugland, Proc. Natl. Acad. Sci. US 58 (1967) 719.

[13] T.S. Rahman, R.S. Knox and V.M. Kenkre, Chem. Phys. 44 (1979) 197.

[14] P.F. Byrd and M.D. Friedman, Handbook of elliptic integrals for engineers and scientists, 2nd Ed. (Springer, Berlin, 1971).

[15] G.P. Tsironis and V.M. Kenkre, Phys. Letters A 127 (1988) 209.

[16] J.C. Eilbeck, A.C. Scott and P.S. Lomdahl, Chem. Phys. Letters 113 (1985) 29; Physica D 16 (1985) 318.

[17] D.K. Campbell, A.R. Bishop and K. Fesser, Phys. Rev. B 26 (1982) 6828.